Analyst

COMMUNICATION

View Article Online
View Journal | View Issue

Cite this: *Analyst*, 2018, **143**, 5670

Received 18th September 2018,
Accepted 23rd October 2018

DOI: 10.1039/c8an01805g

rsc.li/analyst

Ultrasensitive and simple fluorescence biosensor for detection of the *mecA* gene of *Staphylococcus aureus* by using an exonuclease III-assisted cascade signal amplification strategy†

Qiong Li,[a,b] Danhua Zhou,[b,c] Jiafeng Pan,[b] Zhi Liu*[a] and Junhua Chen *[b]

In this work, a label-free fluorescence biosensor for ultrasensitive and simple detection of the *mecA* gene of *Staphylococcus aureus* was proposed by using an exonuclease III (Exo III)-assisted cascade signal amplification strategy. The 3′ end-extruding hairpin probe (HP) acted as the target recognition element and the caged G-quadruplex was used as the signal reporter. Without the *mecA* gene, the HP probe cannot be digested by Exo III, as the G-rich sequences are blocked in the stem of the HP probe. In the presence of the *mecA* gene, the hybridization of the *mecA* gene with the 3′ end-extruding HP probe triggers the digestion reaction of Exo III, liberating the *mecA* gene and the *mecA* gene analogue. Both the released *mecA* gene and the *mecA* gene analogue can hybridize with other HP probes and activate another round of the cleavage reaction. Consequently, the released free G-quadruplex is "lit up" by *N*-methylmesoporphyrin IX (NMM), displaying a dramatically enhanced fluorescence intensity. This sensing platform showed a high sensitivity towards the *mecA* gene with a detection limit as low as 2.4 fM without any labelling, immobilization, or washing steps. The designed sensing system also exhibits excellent selectivity for the *mecA* gene in the presence of other interfering DNA sequences. Furthermore, the presented biosensor is robust and has been successfully applied for the detection of the *mecA* gene in a real food sample with satisfactory results. Owing to its simplicity, cost-effectiveness and ultrasensitivity, our proposed sensing strategy provides a promising platform for the detection of other genes by substituting the target-recognition element.

Introduction

Staphylococcus aureus (*S. aureus*) is one of the most worrying foodborne bacteria as it is ubiquitous in the environment and food samples.[1–3] It can cause severe adverse effects on human health and animals even at low concentrations,[4–7] such as pneumonia, septicemia, toxic shock syndrome, osteomyelitis, and endocarditis.[8] Therefore, the development of a simple highly sensitive biosensor for *S. aureus* detection is urgently needed.

Conventional methods for the detection of *S. aureus* are primarily based on bacteria isolation, and include microarray,[9,10] polymerase chain reaction (PCR),[11,12] next generation sequencing (NGS),[13] enzyme-linked immune-absorbent assay (ELISA),[14] and surface plasmon resonance (SPR) methods.[15] Even though these methods could give accurate results, they are expensive, time-consuming, and require fussy pre-treatment. Thus, it is of great significance to design a convenient, rapid, and low-cost detection approach for *S. aureus* analysis. Until now, biosensors have been widely used for foodborne bacteria detection,[16–19] such as colorimetric biosensors,[20,21] electrochemical biosensors[22,23] and fluorescence biosensors.[24] However, most of them exhibit relativity poor sensitivity and require conditions to be controlled, which inhibits application of these technologies. To overcome these limitations, the Exo III-assisted signal amplification strategy has been applied.[25–27] Unlike other endonucleases,[28–31] Exo III is a sequence-independent enzyme that does not require a specific recognition site and can catalyze the stepwise removal of mononucleotides from the 3-hydroxyl terminus of duplex DNA in the case of substrates which have a blunt or recessed 3′ terminus. Its activity on single-stranded DNA (ssDNA) or double stranded DNA (dsDNA) with a protruding 3′ end is limited.[32–34] Therefore, Exo III provides a versatile platform for the amplified detection of nucleic acids.

G-quadruplexes are structures that are formed by stacked G-tetrads, a planar association of four guanines by Hoogsteen hydrogen bonding.[35] Owing to their structural polymorphism

[a]*College of Bioscience and Biotechnology, Hunan Agricultural University, Changsha 410128, China. E-mail: tigerzhiliu@126.com*
[b]*Guangdong Key Laboratory of Integrated Agro-environmental Pollution Control and Management, Guangdong Institute of Eco-Environmental Science & Technology, Guangzhou 510650, China. E-mail: 222chenjunhua@163.com, jhchen@soil.gd.cn*
[c]*College of Natural Resources and Environment, South China Agricultural University, Guangzhou 510642, China*

† Electronic supplementary information (ESI) available: Fig. S1–S3 and Table S1. See DOI: 10.1039/c8an01805g

and tunable conformation, G-quadruplexes have been widely used as building blocks for directing the assembly of nanoscale components into sophisticated structures or as a functional tool for constructing nanoscale devices and biosensors.[36–38] *N*-Methyl mesoporphyrin IX (NMM) is a commercially available unsymmetrical anionic porphyrin characterized by a pronounced structural selectivity for G-quadruplex, but not for duplex (DNA, RNA and RNA-DNA hybrid), triplex or single-stranded forms.[39,40] Generally, NMM only shows a weak fluorescence in the free state, but exhibits a 20-fold enhancement in its fluorescence upon interacting with the G-quadruplex.[41]

In this work, a simple, facile, highly sensitive and selective detection method for the *mecA* gene of *S. aureus* was developed using a label-free Exo III-assisted target amplification assay. Briefly, the hybridization of the *mecA* gene with the 3′ end-extruding hairpin probe (HP) probe triggers the digestion reaction of Exo III, liberating the *mecA* gene and the *mecA* gene analogue. Subsequently, both the released *mecA* gene and the *mecA* gene analogue can hybridize with other HP probes and activate another round of the cleavage reaction. Ultimately, the increasing G-quadruplex/NMM complex leads to a dramatic enhancement in the fluorescence intensity. Taking advantage of the signal amplification method, the designed biosensor could achieve a high sensitivity for *mecA* gene detection. Owing to its cost-effectiveness, easy operation, and flexibility, the sensing system could be a promising platform for *mecA* gene detection in environmental monitoring, food control, and clinical diagnostics.

Experimental section

Materials and reagents

Dimethyl sulfoxide (DMSO), and tris-(hydroxymethyl) aminomethane (Tris) were purchased from Sigma-Aldrich (St Louis, Mo). Exo III, which can catalyze the stepwise removal of mononucleotides from the 3′-hydroxyl terminus of double-stranded DNA with a blunt or recessed 3′ termini and shows limited activity on single-stranded DNA or duplex DNA with a protruding 3′ end, was purchased from New England Biolabs (Ipswich, MA). NMM was purchased from Frontier Scientific Inc. (Logan, Utah, USA). A 5 mM NMM stock solution was prepared in DMSO and stored at −20 °C before use. All other reagents and materials were of analytical grade and used without purification. All of the solutions were prepared with ultrapure water (18.2 MΩ cm^{-1}) from a Millipore Milli-Q water purification system (Billerica MA).

All of the DNA oligonucleotides were ULTRAPAGE-purified and were purchased from Shanghai Sangon Biotechnology Co., Ltd (Shanghai, China) and their sequences were listed as follows:

mecA gene: 5′-ATTGGGATCATAGCGTCATT-3′

HP: 5′-GGGTAGGGCGGGTTGGGATTGGGATCATAGCGTCATTGATCCCAATCCCAACCCGCCCTACCCCTATGATCCCAAT-3′

M1: 5′-ATTGGGATGATAGCGTCATT-3′

M2: 5′-ATTGGGATGATACCGTCATT-3′

M3: 5′-ATTGCGATGATACCGTCATT-3′

NC: 5′-TGCCGCTCATCCGCCACATA-3′

Red letters represent the mismatched bases.

Assay procedure

The DNA solution was incubated at 90 °C for 10 min and then gradually cooled to room temperature. The obtained DNA solution was stored at 4 °C for further use.

Various concentrations of the *mecA* gene were then incubated with 300 nM HP and 0.2 unit per μL Exo III with a reaction volume of 40 μL for 50 min at room temperature. Next, 500 nM NMM was introduced to the above solution, and this was further incubated at room temperature for 30 min. Finally, the resulting solutions were diluted to 200 μL. The fluorescence spectra were recorded using an F-7000 spectrometer (Hitachi, Japan) at room temperature. The scanning wavelength ranged from 580 to 680 nm (λ_{ex} = 399 nm, λ_{em} = 610 nm). The fluorescence intensity at 610 nm was used to estimate the performance of the proposed biosensor. The slit widths of both the excitation and emission were 10 nm, and the PMT detector voltage was 700 V. All measurements were performed in 20 mM Tris-HCl buffer (pH = 7.4, 100 mM NaCl, 10 mM $MgCl_2$, 15 mM KCl).

Gel electrophoresis

To prepare the hydrogel, 5 mL of 30% gel solution (29 : 1), 1 mL TBE buffer (10×), 100 μL APS, 4 μL TEMED, and 3.8 mL deionized water were mixed together. This mixture contained a final gel percentage of 15%. The gel was polymerized for 1.5 h at room temperature and then soaked in a 1× TBE buffer prior to use. 5 μL of each reacted sample was mixed with 1 μL of 6× loading buffer and was subject to 15% non-denaturing polyacrylamide gel electrophoresis (PAGE). The PAGE was carried out in 1× TBE at a constant voltage of 70 V for about 60 min at room temperature. After staining in diluted SYBR gold solution, the gels were scanned using a Gel Doc XR documentation system (Bio-RAD Laboratories Inc. USA).

Results and discussion

Strategy for *mecA* gene monitoring

The strategy for the amplified detection of *mecA* gene on the basis of the Exo III-assisted cascade signal amplification strategy is schematically demonstrated in Scheme 1. We used a HP probe as the target recognition element and the caged G-quadruplex was used as the signal reporter. The HP probe includes four functional regions. Region 1 (at the 5′ termination) contains the caged G-rich sequence. Region 2 incorporates a similar sequence to the *mecA* gene. When the HP probe is digested by Exo III, region 1 and region 2 can form a *mecA* gene analogue to start another round of amplification. Region 3 acts as a "stabilizer" to steady the HP probe structure. Region 4 (at the 3′ termination) can hybridize with the *mecA* gene and the *mecA* analogue through base pairing. In the pres-

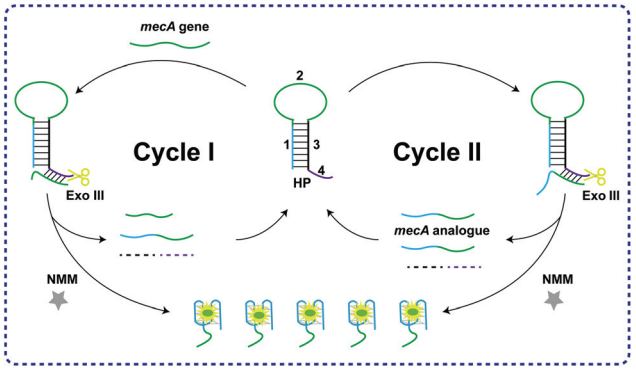

Scheme 1 Schematic representation of the design strategy for the amplified detection of the *mecA* gene on the basis of an Exo III-assisted cascade signal amplification strategy.

ence of the *mecA* gene, the combination of the *mecA* gene and region 4 of the HP probe leads to the *mecA* gene/HP complex which has a blunt 3′ terminus. This complex triggers the digestion reaction of Exo III, liberating the *mecA* gene and the *mecA* gene analogue. Both the *mecA* gene and the *mecA* gene analogue can hybridize with other HP probes and activate another round of the hydrolysis reaction, respectively. Finally, the free G-rich sequence produced can form a G-quadruplex structure, which can be "lit up" by NMM, exhibiting a dramatically increased fluorescence.[42] In the absence of the *mecA* gene, the 3′ end-protruding HP probe cannot be digested by Exo III, as the Exo III only cleaves dsDNA with a blunt or recessed 3′ terminus.[43–45] Therefore, the G-rich sequence is still caged in the HP probe. Thus, the system only yields a relatively low fluorescence background. Most importantly, the sensing system, using G-quadruplex/NMM as the signal reporter, avoids the use of any labels or modification procedures.

Feasibility study

To verify the ability of the designed autocatalytic DNA machine for target detection, the fluorescence spectra were investigated under different conditions. As shown in Fig. 1a, when the HP probe was alone in the solution, it exhibited a weak fluorescence emission peak at 610 nm (black curve), implying that when the G-rich sequence was caged in the HP probe, the NMM cannot interact with the G-rich sequence. When both the HP probe and Exo III were present, the fluorescence intensity was slightly enhanced compared with the background fluorescence signal (pink curve). Without Exo III (blue curve) the solution exhibited a very weak fluorescence as with the black and pink curve. In the presence of *mecA* gene, HP probe, and Exo III, the fluorescence intensity improved sharply (red curve), suggesting that the *mecA* gene/HP complex (with a 3′-blunt termini) was formed and digested by Exo III. The G-rich sequence was released and then interacted with the fluorescence dye NMM. These results gave strong evidence that our designed sensing system can feasibly provide an amplified fluorescence signal for the detection of the target *mecA* gene.

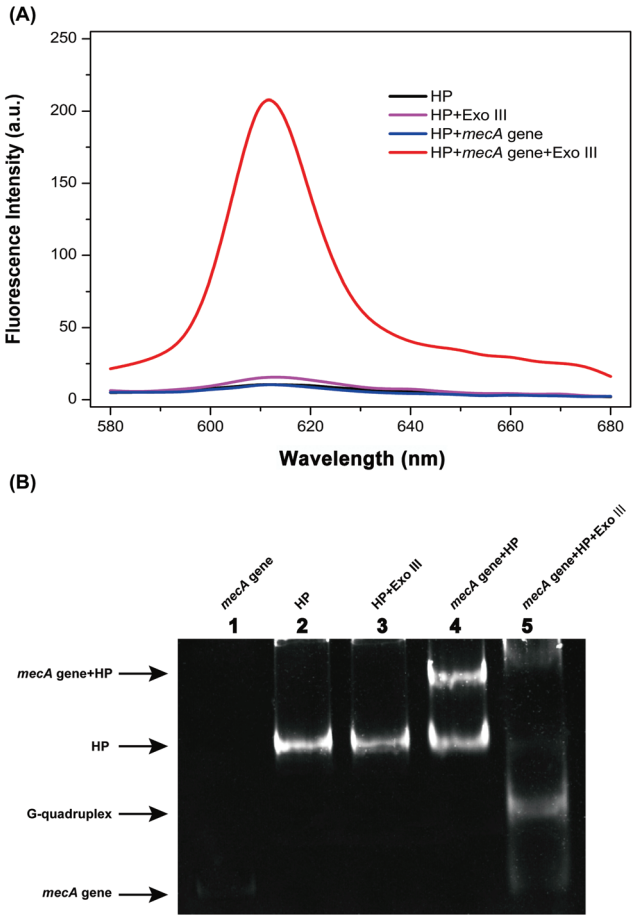

Fig. 1 (a) Fluorescence spectra of the system under different conditions. HP: 300 nM; NMM: 500 nM; Exo III: 0.2 unit per μL; (B) the PAGE images of lane 1: *mecA* gene; lane 2: HP; lane 3: HP + Exo III; lane 4: *mecA* gene + HP; and lane 5: *mecA* gene + HP + Exo III. HP: 3 μM. The experiments were performed at room temperature (25 °C).

To further verify the feasibility of this study, PAGE was used to confirm the results of the fluorescence assay. The electrophoresis results are shown in Fig. 1b.

Obviously, the HP probe was not hydrolyzed by Exo III (lane 3). However, after the *mecA* gene hybridizes with the HP probe (lane 4), it is digested by Exo III, and releases the *mecA* gene and the *mecA* gene analogue (containing the G-quadruplex) (lane 5). The above results further indicate that our designed detecting system can be utilized for the amplified detection of the target *mecA* gene.

Optimization of this assay

The experimental parameters (such as the temperature, the reaction time, and the concentration of Exo III) that could affect the analytical performance of the designed sensing system were optimized. The optimizations were performed by varying one experimental condition and keeping the conditions of the other parameters constant. In our study, the reaction temperature plays an important role in the sensing process. It not only effects the binding kinetics between the

HP probe and the target *mecA* gene, but also the activity of Exo III. The effect of reaction temperature on the response of the fluorescence sensor was investigated by detecting 10 nM of the *mecA* gene at different temperatures (4, 25, 37, and 45 °C). The blank sample (in the absence of the *mecA* gene) at each temperature was tested under the same conditions. As shown in Fig. S1 (ESI†), the fluorescence signal increased with the increase in the temperature (4–37 °C) in the presence of the *mecA* gene (10 nM). However, the fluorescence intensity decreased when the temperature continued to rise (37–45 °C) (green histogram in Fig. S1, ESI†). On the one hand, the higher temperature may change the conformation of the HP probe, which increases the background signal.[46] On the other hand, the activity of Exo III may be deactivated. In order to obtain the best signal-to-background ratio (S/N) (red line in Fig. S1, ESI†), 25 °C was considered to be the optimum reaction temperature. The corresponding error bars in Fig. S1† represent the standard deviation of the three independent measurements obtained at each reaction temperature.

The performance of the signal amplification and detection of the *mecA* gene was deeply influenced by the reaction time of the Exo III. In order to optimize the reaction time, we controlled the fluorescence signal response at 25 °C. As shown in Fig. S2 (ESI†), the fluorescence intensity of the solution containing 10 nM of the *mecA* gene increased rapidly when the incubation time ranged from 10 to 30 min and remained at almost a constant level after 30 min, which suggested that the G-rich sequence was almost completely released from the HP probe for the formation of the G-quadruplex/NMM complex. Therefore, 30 min was selected as the optimum reaction time.

The effect of the concentration of Exo III was also taken into consideration. As shown in Fig. S3 (ESI†), the S/N level increased gradually with the increasing concentration of Exo III from 0.1 to 0.15 unit per μL, and reached a peak at 0.15 unit per μL. However, the S/N level decreased when the Exo III concentration continued to rise (0.15–0.3 unit per μL). The decreased S/N at higher concentrations of Exo III can be ascribed to the fact that too many enzymes would cleave the HP probe even in the absence of the target, resulting in a relatively high background signal. Thus, 0.15 unit per μL Exo III was chosen for further experiments.

Analytical performance of the biosensor

To investigate the dynamic range and sensitivity of the assay, a series of samples containing different concentrations of the *mecA* gene were tested under optimal experimental conditions. As shown in Fig. 2a, the fluorescence intensity was enhanced as the concentration of the *mecA* gene increased (0–1 μM). The relationship between the fluorescence intensity at 610 nm and the concentration of the *mecA* gene is displayed in Fig. 2b. The resulting calibration curve shows that a linear dependence between the fluorescence intensity and the logarithm of the *mecA* gene concentration was obtained in the range from 10 fM to 100 nM with a correlation coefficient (R^2) of 0.99 (Fig. 2b, inset). The linear regression equation is $y = 24.94 \lg C + 16.25$ (y and C represent the fluorescence peak intensity and the concentration of the *mecA* gene, respectively). According to the 3δ rule,[47] the calculated limit of detection (LOD) is 2.4 fM. Compared with the previously reported method of *mecA* gene detection, our sensing platform proposed demonstrated a greater sensitivity (Table S1, ESI†). Such a high sensitivity could be attributed to the fact that the autocatalytic DNA machine can stimulate the formation of numerous G-quadruplex/NMM complexes even at a low concentration of the target *mecA* gene. Here, our proposed fluorescence detection strategy holds great potential for monitoring of the *mecA* gene in real food samples with high sensitivity.

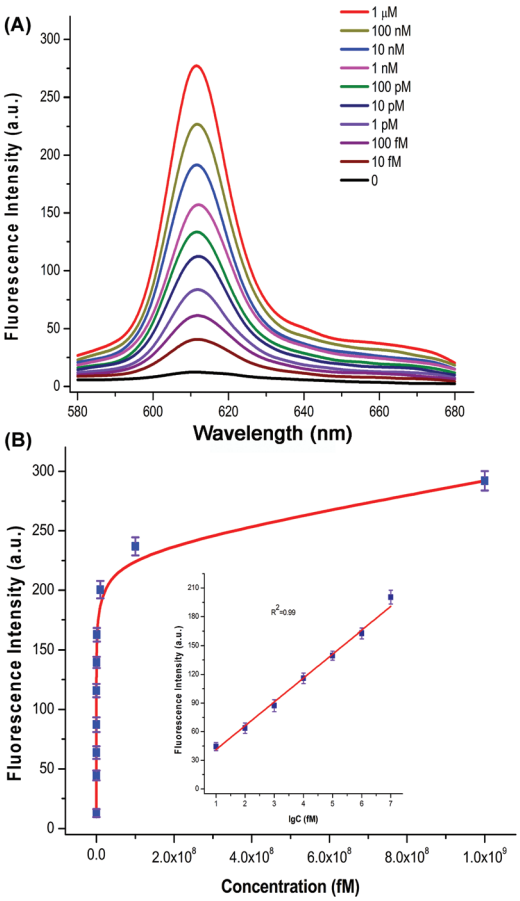

Fig. 2 (A) Fluorescence spectra upon addition of different concentrations of the *mecA* gene. (B) Plots of the fluorescence intensity at 610 nm as a function of the *mecA* gene concentration. Inset: Linear relationship between the fluorescence intensity and the logarithm of the *mecA* gene concentration in the range from 10 fM to 100 nM. The corresponding error bars in (b) represents the standard deviation of three independent measurements obtained at different concentrations of the *mecA* gene.

The selectivity of the sensing platform for the *mecA* gene to four other kinds of DNA sequences, including a single-base mismatched DNA (M1), a two base mismatched DNA (M2), a three base mismatched DNA (M3), and the non-complementary DNA (NC) at the same concentration of 10 nM, were also analyzed using the present sensing system. As shown in Fig. 3, the fluorescence intensity varies with the target and the four

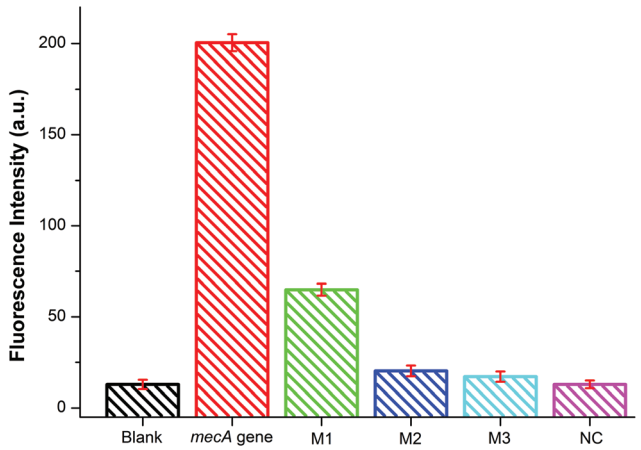

Fig. 3 Selectivity of the sensing system analyzing the *mecA* gene against other four different kinds of DNA sequences. The concentration was 10 nM for the *mecA* gene and the four other DNA sequences. The corresponding error bars represent the standard deviation of three independent measurements obtained for different analytes.

Table 1 Analysis of real samples containing the *mecA* gene at different concentrations

Sample	Added (pM)	Found[a] (pM)	Recovery (%)	RSD (%)
Milk sample 1	0.01	0.0086	86%	7.6
Milk sample 2	0.1	0.96	96%	6.4
Milk sample 3	1	1.02	102%	3.8

[a] The data reported in the table represents the average of five measurements.

other kinds of DNA. The relative fluorescence intensity for M1 and M2 were about 32% and 1% of the *mecA* gene, respectively. The M3 and NC showed almost the same intensity as the blank sample. These results clearly demonstrated the high specificity of our designed sensing system.

Real sample analysis

To investigate whether this fabricated monitoring system could be applied to real samples, a recovery experiment was carried out. Milk samples, purchased from a local market, were spiked with different concentrations, 0.01, 0.1, 1 pM, of the *mecA* gene. As shown in Table 1, the recovery of all of the measured samples and the relative standard derivations (RSD) were in the ranges from 86–102% and 3.8–7.6% (n = 5), respectively, which indicated that the possible interference from the milk sample to the biosensor analysis was negligible. This above data proved that our designed method can be successfully applied for the detection of the *mecA* gene in real food samples.

Conclusions

In conclusion, a facile, isothermal, and ultrasensitive platform for the detection of the *mecA* gene of *S. aureus* was developed by using an Exo III-assisted target recycling and G-quadruplex/NMM cascade signal amplification strategy. Firstly, we employed a HP probe to achieve recognition of the *mecA* gene. Then, the detection signal can be exponentially produced using Exo III-assisted cascade target recycling. Finally, the increasing G-quadruplex interacts with NMM to form G-quadruplex/NMM complexes, which result in an enhanced fluorescence intensity of the reaction solution for the highly sensitive detection of the *mecA* gene at concentrations as low as 2.4 fM. Moreover, the designed sensor also exhibits an excellent selectivity toward the *mecA* gene compared with other interfering DNA samples. Furthermore, this method can be applied for the determination of the *mecA* gene in spiked real food samples with good recovery and accuracy. Without the use of any labeling, immobilization, washing, or modification steps, the developed method described herein is easy to apply for routine monitoring of the *mecA* gene. Importantly, the designed autocatalytic DNA machine could be easy extended to fabricate versatile and robust sensing platforms for the detection of other genes by choosing the corresponding recognition elements. With the characteristics described above, this biosensor and autocatalytic DNA machine has great promise for application as a platform for foodborne pathogen monitoring for environmental monitoring, food control and clinical diagnostics.

Conflicts of interest

There are no conflicts to declare.

Acknowledgements

Financial support was provided by the Guangdong National Science Funds for Distinguished Young Scholars (2016A030306012), the NSFC (31671933), the Local Innovative and Research Teams Project of the Guangdong Pearl River Talents Program (2017BT01Z176), and the Science and Technology Planning Project of Guangdong Province (2017A070702015 and 2017B030314092).

Notes and references

1 M. Z. David and R. S. Daum, *Clin. Microbiol. Rev.*, 2010, **23**, 616–687.
2 T. Miao, Z. Wang, S. Li and X. Wang, *Microchim. Acta*, 2011, **172**, 431–437.
3 M. Rubab, H. M. Shahbaz and A. N. Olaimat, *Biosens. Bioelectron.*, 2018, **105**, 49–57.
4 B. Pinto, E. Chenoll and R. Aznar, *Syst. Appl. Microbiol.*, 2005, **28**, 340–352.
5 J. M. Soriano, G. Font, J. C. Moltó and J. Mañes, *Trends Food Sci. Technol.*, 2002, **13**, 60–67.
6 P. Leonard, S. Hearty, J. Brennan, L. Dunne, J. Quinn, T. Chakraborty and R. O'Kennedy, *Enzyme Microb. Technol.*, 2003, **32**, 3–13.
7 K. Zhang, J. A. McClure and S. Elsayed, *J. Clin. Microbiol.*, 2005, **43**, 5026–5033.

8 R. J. Gorwitz, D. Kruszon-Moran and S. K. McAllister, *J. Infect. Dis.*, 2008, 1226–1234.
9 T. Wang, Z. Zhang and Y. Li, *Sens. Actuators, B*, 2015, **221**, 148–154.
10 M. Bally, M. Halter, J. Voros and H. M. Grandin, *Surf. Interface Anal.*, 2006, **38**, 1442–1458.
11 M. Kuroda, T. Ohta and I. Uchiyama, *Lancet*, 2001, **357**, 1225–1240.
12 B. Alarcon, B. Vicedo and R. Aznar, *J. Appl. Microbiol.*, 2006, **100**, 352–364.
13 S. P. Yazdankhah, A. L. Hellemann, K. Rønningen and E. Olsen, *Vet. Microbiol.*, 1998, **62**, 17–26.
14 S. S. Oh, K. Plakos, X. Lou, Y. Xiao and H. T. Soh, *Proc. Natl. Acad. Sci. U. S. A.*, 2010, **107**, 14053–14058.
15 H. Zhang, X. Ma, Y. Liu, N. Duan, S. Wu, Z. Wang and B. Xu, *Biosens. Bioelectron.*, 2015, **74**, 872–877.
16 E. C. Alocilja and S. M. Radke, *Biosens. Bioelectron.*, 2003, **18**, 841–846.
17 L. Yang, Y. Li, C. L. Griffis and M. G. Johnson, *Biosens. Bioelectron.*, 2004, **19**, 1139–1147.
18 J. Yu, Z. Liu, Q. Liu and K. T. Yuen, *Sens. Actuators, A*, 2009, **154**, 288–294.
19 K. Y. Chan, W. W. Ye and Y. Zhang, *Biosens. Bioelectron.*, 2013, **41**, 532–537.
20 W. C. Lindsey, E. S. Woodruff, D. Weed, D. C. Ward and R. D. Jenison, *Diagn. Microbiol. Infect. Dis.*, 2008, **61**, 273–279.
21 J. Klonoski, R. Mondesire, L. Rea, D. C. Ward and R. D. Jenison, *Anal. Biochem.*, 2010, **396**, 284–289.
22 M. Liu, H. Xiang, E. Hua and L. Wang, *Anal. Lett.*, 2014, **47**, 579–591.
23 L. Xu, W. Liang and Y. Wen, *Biosens. Bioelectron.*, 2018, **99**, 424–430.
24 J. Shi, C. Chan, Y. Pang and W. Ye, *Biosens. Bioelectron.*, 2015, **67**, 595–600.
25 Y. Gao and B. Li, *Anal. Chem.*, 2014, **86**, 8881–8887.
26 S. Liu, C. Cheng, T. Liu, L. Wang, H. Gong and F. Li, *Biosens. Bioelectron.*, 2015, **63**, 99–104.
27 W. Li, X. Liu, T. Hou, H. Li and F. Li, *Biosens. Bioelectron.*, 2015, **70**, 304–309.
28 X. Liu, W. Li, T. Hou, S. Dong, G. Yu and F. Li, *Anal. Chem.*, 2015, **87**, 4030–4036.
29 T. Hou, X. Wang, X. Liu, T. Lu, S. Liu and F. Li, *Anal. Chem.*, 2013, **86**, 884–890.
30 L. Ge, W. Wang, X. Sun, T. Hou and F. Li, *Anal. Chem.*, 2016, **88**, 2212–2219.
31 X. Liu, M. Chen, T. Hou, X. Wang, S. Liu and F. Li, *Biosens. Bioelectron.*, 2014, **54**, 598–602.
32 C. Fu, C. Liu, Y. Li, Y. Guo, F. Luo, P. Wang, L. Guo, B. Qiu and Z. Lin, *Anal. Chem.*, 2016, **88**, 10176–10182.
33 X. Liu, R. Freeman and I. Willner, *Chem. – Eur. J.*, 2012, **18**, 2207–2211.
34 E. Xiong, X. Yan, X. Zhang, Y. Liu, J. Zhou and J. Chen, *Biosens. Bioelectron.*, 2017, **87**, 732–736.
35 D. Hu, Z. Huang, F. Pu, J. Ren and X. Qu, *Chem. – Eur. J.*, 2011, **17**, 1635–1164.
36 H. Li, J. Chang, P. Gai and F. Li, *ACS Appl. Mater. Interfaces*, 2018, **10**, 4561–4568.
37 F. Pu, Z. Huang, D. Hu, J. Ren, S. Wang and X. Qu, *Chem. Commun.*, 2009, 7357–7359.
38 T. Hou, W. Li, X. Liu and F. Li, *Anal. Chem.*, 2015, **87**, 11368–11374.
39 J. Ren and J. B. Chaires, *Biochemistry*, 1999, **38**, 16067–16075.
40 H. Li, J. Chang, T. Hou and F. Li, *Anal. Chem.*, 2017, **89**, 763–680.
41 J. Zhao, C. Chen, L. Zhang, J. Jiang, G. Shen and R. Yu, *Analyst*, 2013, **138**, 1713–1718.
42 D. Hu, Z. Huang, F. Pu, J. Ren and X. Qu, *Chem. – Eur. J.*, 2011, **17**, 1635–1641.
43 C. Shi, C. Zhao, Q. Guo and C. Ma, *Chem. Commun.*, 2011, **47**, 2895–2897.
44 X. Wang, X. Liu, T. Hou, W. Li and F. Li, *Sens. Actuators, B*, 2015, **208**, 575–580.
45 J. Chen, S. Zhou and J. Wen, *Anal. Chem.*, 2014, **86**, 3108–3114.
46 J. Chen and S. Zhou, *Biosens. Bioelectron.*, 2016, **77**, 277–283.
47 J. Yin, Y. Liu and S. Wang, *Sens. Actuators, B*, 2018, **256**, 573–579.